

# Accepted Manuscript

A near-infrared fluorescent probe based on  $S_NAr$  reaction for  $H_2S$ /GSH detection in living cells and zebrafish

Han Zhang, Xiang Xia, Hong Zhao, Guo-Ning Zhang, Dao-Yong Jiang, Xing-Ying Xue, Jiao Zhang

PII: S0143-7208(18)32256-3

DOI: <https://doi.org/10.1016/j.dyepig.2018.11.050>

Reference: DYPI 7194

To appear in: *Dyes and Pigments*

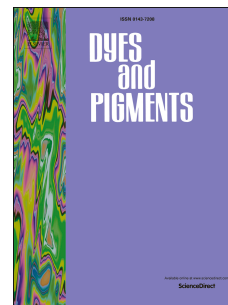
Received Date: 10 October 2018

Revised Date: 14 November 2018

Accepted Date: 24 November 2018

Please cite this article as: Zhang H, Xia X, Zhao H, Zhang G-N, Jiang D-Y, Xue X-Y, Zhang J, A near-infrared fluorescent probe based on  $S_NAr$  reaction for  $H_2S$ /GSH detection in living cells and zebrafish, *Dyes and Pigments* (2018), doi: <https://doi.org/10.1016/j.dyepig.2018.11.050>.

This is a PDF file of an unedited manuscript that has been accepted for publication. As a service to our customers we are providing this early version of the manuscript. The manuscript will undergo copyediting, typesetting, and review of the resulting proof before it is published in its final form. Please note that during the production process errors may be discovered which could affect the content, and all legal disclaimers that apply to the journal pertain.



# A near-infrared fluorescent probe based on $S_NAr$ reaction for $H_2S$ /GSH detection in living cells and zebrafish

Han Zhang,<sup>a,†</sup> Xiang Xia,<sup>a,†</sup> Hong Zhao,<sup>a,\*</sup> Guo-Ning Zhang,<sup>b</sup> Dao-Yong Jiang,<sup>a</sup> Xing-Ying Xue,<sup>a</sup> Jiao Zhang,<sup>a</sup>

<sup>a</sup> School of Chemistry and Chemical Engineering, Southeast University, Nanjing, 211189, China.

†: Han Zhang and Xiang Xia contributed equally to this work.

Corresponding author E-mail adress: [zhaohong@seu.edu.cn](mailto:zhaohong@seu.edu.cn)

## Abstract

Hydrogen sulfide ( $H_2S$ ) and biothiols such as cysteine (Cys), homocysteine (Hcy) and glutathione (GSH), play critical roles in physiological and pathological processes. However, due to the challenge in sensing  $H_2S$  and biothiols simultaneously, it is of great importance to solve this problem in biological processes. Herein, a near-infrared fluorescent probe (HZ-NBD) based on  $S_NAr$  reactions was exploited to achieve the sensitive and selective detection of  $H_2S$  and glutathione (GSH) simultaneously in the same conditions. The design strategy was employing dicyanoisophorone based fluorescent dye as the fluorophore, the NBD moiety as a response unit and a quencher of fluorophore. The probe exhibited a low limit of detection to  $H_2S$  (13.2 nM) and GSH (112 nM) as well as a favorable large stokes shift (112 nm). The reaction mechanism was investigated via mass spectra. What's more, owing to the advantages of low cytotoxicity, fast response and strong anti-interference ability, the probe HZ-NBD was successfully applied to bioimage  $H_2S$  and GSH in HepG2 cells and zebrafish.

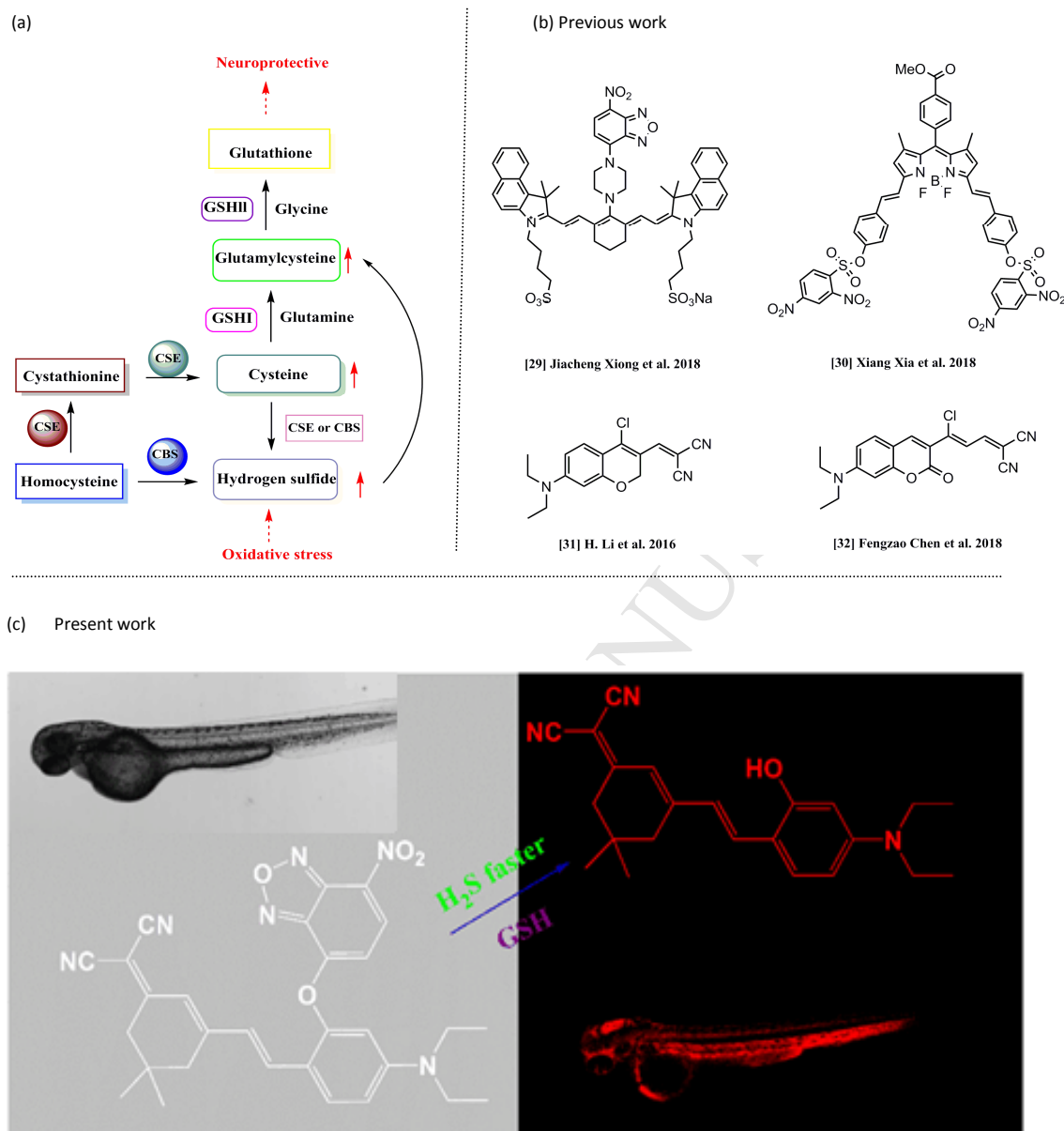
**Key words:** dicyanoisophorone, near-infrared emission,  $S_NAr$ , fluorescent probe

## 1. Introduction

Hydrogen sulfide ( $H_2S$ ) and biothiols such as cysteine (Cys), homocysteine (Hcy) and glutathione (GSH), play crucial roles in many physiological processes[1-4]. Generally speaking, In living organism, the endogenous  $H_2S$  can be produced from cysteine (Cys) and homocysteine (Hcy) by cystathionine- $\gamma$ -lyase (CES), cystathionine- $\beta$ -synthase (CBS), and 3-mercaptopyruvate sulfurtransferase (3-MST), which exists in the cardiovascular system, liver, kidneys and brain[5-7]. What's more, a series of studies have demonstrated that it is not the  $H_2S$  that performs straightly as an antioxidant to protect neurons from oxidative stress, it achieves neuromodulation via adding the level of GSH.  $H_2S$  itself can't rescue cells from oxidative stress but it could induce the generation of a major and potent antioxidant GSH[8, 9]. Notably, there is a close correlation between the physiological level of biothiols and  $H_2S$  (Fig.S1)[10]. However, the abnormal amounts of  $H_2S$  and GSH are related to some human diseases. For example, abnormal production of  $H_2S$  may cause human diseases including diabetes, Alzheimer's disease and Down syndrome and the concentration of GSH is directly linked to cancer, cardiovascular disease and Alzheimer's disease[11-14]. Hence, it is urgently required to develop sensitive and selective methods to monitor  $H_2S$  and GSH for the early diagnosis and therapy of some related diseases.

Fluorescent probes have gained more and more attention due to their sensitivity, selectivity, simplicity and real-time detection[15-19]. To date, various fluorescent probes have been developed for the detection of  $H_2S$  or GSH[20-28]. For instance, Xiong et al.[29] have reported a NIR fluorescent probe based on cyanine for  $H_2S$  and Xia et al.[30] have synthesized a BODIPY-based turn on fluorescent probe with red emission to discriminate GSH over Cys and Hcy. Encouragingly, further efforts have been contributed to discover a single probe for the synchronous detection of  $H_2S$  and GSH. On the basis of coumarin, Li et al.[31] and Chen et al. [32] designed two fluorescent probe, which achieved the simultaneous detection of  $H_2S$  and GSH. Nevertheless, limitations such as short emission wavelength, still exist in previously reported probe, which greatly restricts their biological applications. To avoid that, the design and implementation of near-infrared (NIR, 650~900 nm) fluorescent probes are of crucial importance, which have admirable merits (deep tissue penetration, low background interference and minimum photo damage) for monitoring the target molecule in vivo and in vitro[33-38]. Therefore, it is of great value to develop a NIR fluorescent probe for simultaneous

detection of H<sub>2</sub>S and GSH.



Scheme. 1(a) The relation diagram among H<sub>2</sub>S, biothiols generation and metabolic pathways. (b) Previous work: recent reports for the detection of H<sub>2</sub>S and GSH simultaneously. (c) Present work: a fluorescent probe for detection of H<sub>2</sub>S/GSH in zebrafish imaging photograph.

Keeping the above in perspective, a near-infrared fluorescent probe HZ-NBD for the simultaneous detection of H<sub>2</sub>S/GSH was exploited. It is well known that the dicyanoisophorone based dyes is used as a colour reporting group owing to its eminent optical properties and biocompatibility[39-42], and 4-aromatic hydroxyl NBD derivatives can be used to distinguish Cys/Hcy from GSH and H<sub>2</sub>S[43-46]. Utilizing the isophorone-based fluorescent dye as the fluorophore, the NBD moiety as a response unit and a quencher of fluorophore, a NIR emission fluorescent probe HZ-NBD

was exploited. As expected, the probe HZ-NBD itself showed negligible fluorescence, while a remarkable fluorescence enhancement at 672 nm appeared via the sulfhydryl-promoted  $S_NAr$  reaction in the presence of  $H_2S$ /GSH. Compared to the previously reported probe, the probe HZ-NBD exhibited many merits as follows: the synchronous discrimination of  $H_2S$ /GSH; emission in the NIR light region; simple synthetic route; high sensitivity with a detection limit of 13.2 nM ( $H_2S$ ) and 112 nM (GSH). Apart from that, the probe HZ-NBD achieved the “naked-eye” detection. Finally, the probe HZ-NBD realized the bioimage of  $H_2S$  and GSH in HepG2 cells and zebrafish with low cytotoxicity.

## 2. Experimental section

### 2.1 Materials and methods

All reagents and solvents were commercially purchased. Solvents were purchased from Sinopharm Chemical Reagent Co. Ltd (Shanghai, China) and used without further refinement. The 4-chloro-7-nitro-1,2,3-benzoxadiazole (NBD-Cl) was purchased from Adamas and 3-(N,N-diethyl amino) phenol, isophorone and malononitrile were purchased from Sinopharm Chemical Reagent Co. Ltd (Shanghai, China). Glutathione (GSH), cysteine (Cys), and homocysteine (Hcy) were purchased from Macklin Biochemical Co. Ltd (AR, Shanghai, China), Shanghai HuiXing Biochemical Reagent Co., Ltd, and Tokyo Chemical Industry Co., Ltd (AR, Shanghai, China), respectively. Histidine (His), aspartic acid (Asp), threonine (Thr), tyrosine (Tyr), lysine (Lys), glutamic acid (Glu), glycine (Gly), Valine (Val), phenylalanine (Phe), Leucine (Leu), proline (Pro), Sodium Chloride (NaCl), Sodium fluoride (NaF), Sodium iodide (NaI), Sodium hypochlorite (NaClO), Sodium sulfate ( $Na_2SO_4$ ), Sodium nitrate ( $NaNO_3$ ), Sodium Carbonate ( $Na_2CO_3$ ) and Sodium Acetate (AcONa) were purchased from Sinopharm Chemical Reagent Co. Ltd (AR, Shanghai, China). Sodium Hydrogen Sulfite ( $NaHSO_3$ ) and Sodium hydrosulfide (NaSH) were purchased from Aladdin (AR, Shanghai, China). A stock solution ( $1 \times 10^{-3} M$ ) of HZ-NBD was prepared in THF and then diluted to the desired concentration prior to the spectroscopic measurements. The various analytes were dissolved in double-distilled water and its stock solution concentration was  $1 \times 10^{-2} M$ .

$^1H$  NMR and  $^{13}C$  NMR spectra were recorded on a Bruker DMX600 NMR spectrometer using  $CDCl_3$  as solvents for dissolving the samples and tetramethylsilane (TMS) as the internal standard. The mass spectra were obtained using an Ultraflex II (MALDI-TOF) spectrometer.

UV-visible absorption spectra were determined on a Shimadzu UV-3600 spectrophotometer. Fluorescence spectra were measured on a HORIBA FL-4 Max spectrometer;  $3 \times 1 \times 1$  cm quartz cuvettes were used for recording absorption and emission spectra. Fluorescence imaging of cells was performed using confocal microscopy (OLMPUS, FV3000). All pH measurements were made on a pHS-3C pH meter and the value of pH of the solution was adjusted by NaOH or HCl. All the measurement experiments were performed at about 298.0 K.

## 2.2 Synthesis of Intermediate compounds and target compound

The synthesis of compound 1 and 2 were prepared according to the references[26, 47].

### 2.2.1 Synthesis of HZ-1

An equal equivalent of 4-(N, N-diethylamino)-2-hydroxybenzaldehyde (2) (0.48 g, 2.5 mmol) and active 2-(3,5,5-trimethylcyclohex-2-enylidene) malononitrile (1) (0.46 g, 2.5 mmol) were heated in a small volume of ethanol under reflux in the presence of a few drops of piperidine catalyst. The reaction progress was monitored by TLC. After the reaction completed, the reaction mixture was cooled and extracted with  $\text{CH}_2\text{Cl}_2$ . Finally, the collected organic layers were dried over anhydrous  $\text{MgSO}_4$ , concentrated under vacuum and purified by silica chromatography (eluted with petroleum/ethyl acetate = 5/1, v/v) to give dark purple powders HZ-1 0.18 g, yield: 20%.  $^1\text{H}$  NMR (600 MHz,  $\text{CDCl}_3$ , TMS):  $\delta$  7.38 (d,  $J$  = 8.8 Hz, 1H), 7.36 (d,  $J$  = 15.9 Hz, 1H), 6.99 (d,  $J$  = 15.9 Hz, 1H), 6.72 (s, 1H), 3.40-3.36 (m, 4H), 2.55 (s, 2H), 2.47 (s, 2H), 1.20 (t,  $J$  = 7.0 Hz, 6H).  $^{13}\text{C}$  NMR (150 MHz,  $\text{CDCl}_3$ , TMS):  $\delta$  169.43, 156.72, 156.53, 129.63, 120.75, 114.58, 113.83, 43.08, 39.16, 29.66, 28.02, 12.66. HRMS calcd for  $\text{C}_{23}\text{H}_{27}\text{N}_3\text{O}$  [HZ-1 + H] $^+$ : 362.21541. Found 362.22121.

### 2.2.2 Synthesis of HZ-NBD

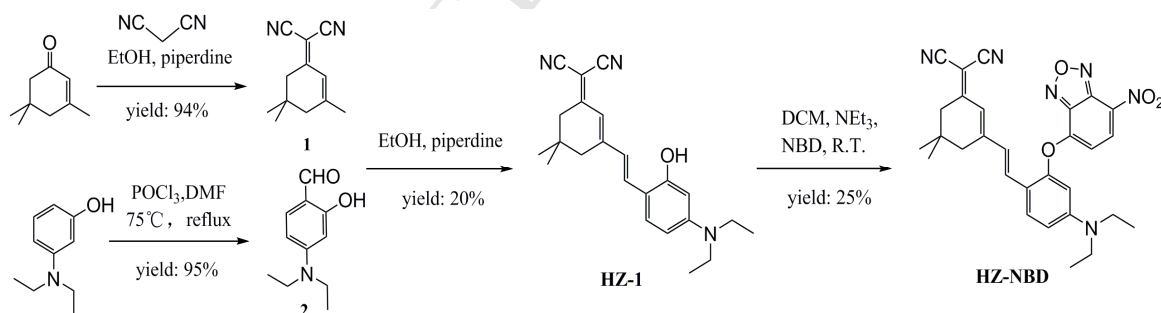
A solution of HZ-1 (0.36 g, 1 mmol), NBD-Cl (0.24 g, 1.2 mmol) and a few drops of  $\text{Et}_3\text{N}$  catalyst in  $\text{CH}_2\text{Cl}_2$  were stirred at room temperature overnight. Then, the mixture solution was evaporated under reduced pressure and purified by silica chromatography (eluted with petroleum/ethyl acetate = 2/1, v/v) to give dark red powders HZ-NBD 0.13 g, yield: 25%.  $^1\text{H}$  NMR (600 MHz,  $\text{CDCl}_3$ , TMS):  $\delta$  8.44 (d,  $J$  = 8.2 Hz, 1H), 7.67 (d,  $J$  = 9.0 Hz, 1H), 6.98 (d,  $J$  = 16.0 Hz, 1H), 6.84 (d,  $J$  = 15.9 Hz, 1H), 6.71-6.70 (m, 2H), 6.54 (d,  $J$  = 8.3 Hz, 1H), 6.36 (d,  $J$  = 2.5 Hz,

1H), 3.42-3.38 (m, 4H), 2.50 (s, 2H), 2.18 (s, 1H), 1.57 (s, 3H), 1.21 (t,  $J = 7.0$  Hz, 6H).  $^{13}\text{C}$  NMR (150 MHz,  $\text{CDCl}_3$ , TMS):  $\delta$  168.94, 154.19, 154.17, 152.98, 150.46, 144.22, 133.37, 130.87, 128.87, 126.67, 122.64, 44.74, 42.93, 38.89, 31.89, 29.66, 27.88, 12.54. HRMS calcd for  $\text{C}_{29}\text{H}_{28}\text{N}_6\text{O}_4$  [HZ-NBD + Na] $^+$ : 547.21720. Found 547.20988.

### 3. Results and discussion

#### 3.1 The design and synthesis of NIR emission fluorescent probe HZ-NBD

A near infrared emission fluorescent probe HZ-NBD has been reported. Herein, utilizing the intermediate 1 as start material, the  $\pi$ -conjugate system was enlarged to NIR region through Knoevenagel condensation reaction by reacting with intermediate 2. Additionally, the HZ-1 presented large Stokes shift (112 nm), meaning that it could be regarded as a favourable platform for the design of NIR fluorescent probe. On the basis, the NBD as a quenching group was introduced. Due to the strong electron-withdrawing ability of NBD, the intramolecular charge transfer (ICT) process was inhibited that caused the quenching of fluorescence. When adding  $\text{H}_2\text{S}$ /GSH, the free fluorophore HZ-1 was produced by a nucleophilic substitution ( $\text{S}_{\text{N}}\text{Ar}$ ) reaction, generating a red emission. Besides, the structures of HZ-NBD and intermediates were confirmed by  $^1\text{H}$  NMR,  $^{13}\text{C}$  NMR and HRMS (Fig. S7-S16).



Scheme. 2 The synthetic route of HZ-NBD

#### 3.2 Specific detection for $\text{H}_2\text{S}$ and GSH

First of all, the selectivity of probe HZ-NBD were examined upon addition of  $\text{H}_2\text{S}$ /GSH and other analytes ( $\text{F}^-$ ,  $\text{Cl}^-$ ,  $\text{ClO}^-$ ,  $\text{I}^-$ ,  $\text{AcO}^-$ ,  $\text{NO}_3^-$ ,  $\text{CO}_3^{2-}$ ,  $\text{SO}_4^{2-}$ ,  $\text{HSO}_3^-$ , Hcy, Cys, His, Asp, Tyr, Lys, Thr, Gly, Phe, Pro, Leu, Ser, Val). As shown in Fig. 1, the probe HZ-NBD itself showed pink colours under sunlight and non-fluorescence with excited at 365 nm by hand UV-lamp, when adding  $\text{H}_2\text{S}$ /GSH, the colour of the solution changed from pink to purple red along with a strong red emission. Besides, according to the Fig. 2, the probe with  $\text{H}_2\text{S}$ /GSH presented a remarkable “off-on” fluorescence signal with a red

emission at 672 nm, while no significant changes were observed with other analytes, especially for Cys and Hcy, which may disturb the detection of H<sub>2</sub>S/GSH. This can be explained by the nucleophilic aromatic substitution (S<sub>N</sub>Ar) reaction promoted by the sulfhydryl group of H<sub>2</sub>S/GSH. Since the NBD group was removed via forming NBD-SH/NBD-S-GSH, the fluorophore HZ-1 was released with NIR emission. As a result, these results proved that HZ-NBD displayed a high selectivity toward H<sub>2</sub>S and GSH. Subsequently, the competition experiments were carried out to further demonstrate the selective recognition of HZ-NBD toward H<sub>2</sub>S and GSH. Upon adding 100 μM H<sub>2</sub>S or GSH into the solution of probe in the presence of 100 μM other analytes (seeing Fig. S1 and S2), the co-existence of other analytes did not interfere with the capability of probe to detect H<sub>2</sub>S and GSH. As a result, these results proved that HZ-NBD displayed a high selectivity toward H<sub>2</sub>S and GSH in the presence of other analytes.

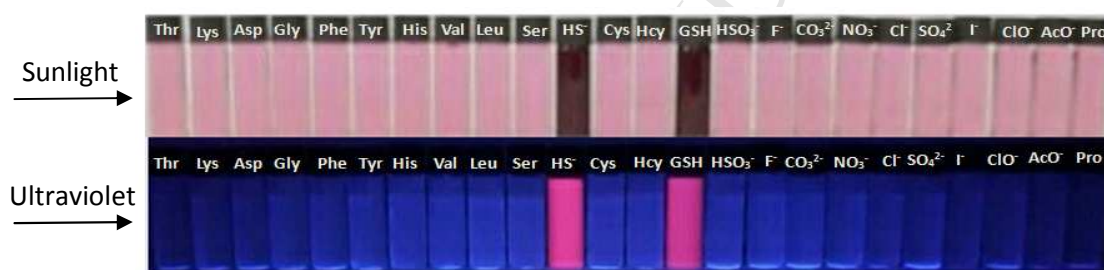


Fig. 1 Photographs of probe HZ-NBD ( $1 \times 10^{-5}$  M) with various analytes (100 μM of NaSH, GSH, Cys, Hcy, His, Tyr, Thr, Lys, Phe, Gly, Trp, Ser, Val, Leu, Pro, HSO<sub>3</sub><sup>-</sup>, Cl<sup>-</sup>, AcO<sup>-</sup>, NO<sub>3</sub><sup>-</sup>, CO<sub>3</sub><sup>2-</sup>, SO<sub>4</sub><sup>2-</sup>, F<sup>-</sup>, I<sup>-</sup>, ClO<sup>-</sup>) were recorded at room temperature. a: sunlight. b: fluorescence observed irradiation with 365 nm.

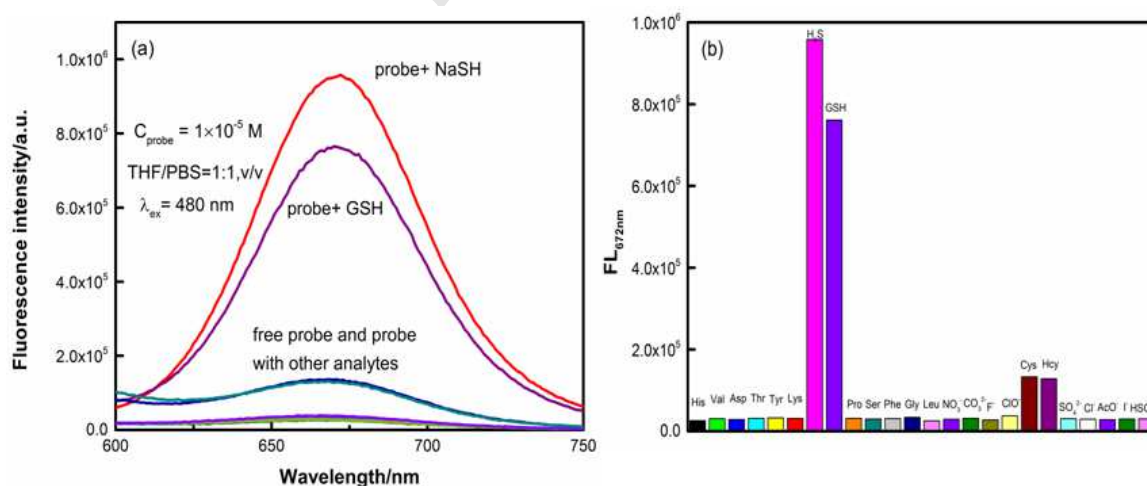


Fig. 2 Fluorescence response of probe HZ-NBD ( $1 \times 10^{-5}$  M) in THF/PBS (v/v 1:1, pH=7.4) mixture solution upon addition of 10 equiv. of NaSH, GSH, Cys, Hcy, His, Tyr, Thr, Lys, Phe, Gly, Trp, Ser, Val, Leu, Pro, HSO<sub>3</sub><sup>-</sup>, Cl<sup>-</sup>, AcO<sup>-</sup>, NO<sub>3</sub><sup>-</sup>, CO<sub>3</sub><sup>2-</sup>, F<sup>-</sup>, I<sup>-</sup>, ClO<sup>-</sup>, SO<sub>4</sub><sup>2-</sup>. (b) The bar graph of fluorescence response at 672 nm of probe HZ-NBD with analytes ( $\lambda_{\text{ex}} = 480$  nm, slit: 3 /3 nm) at r.t.

### 3.3 UV-vis and fluorescence response of HZ-NBD to different concentrations of H<sub>2</sub>S/GSH

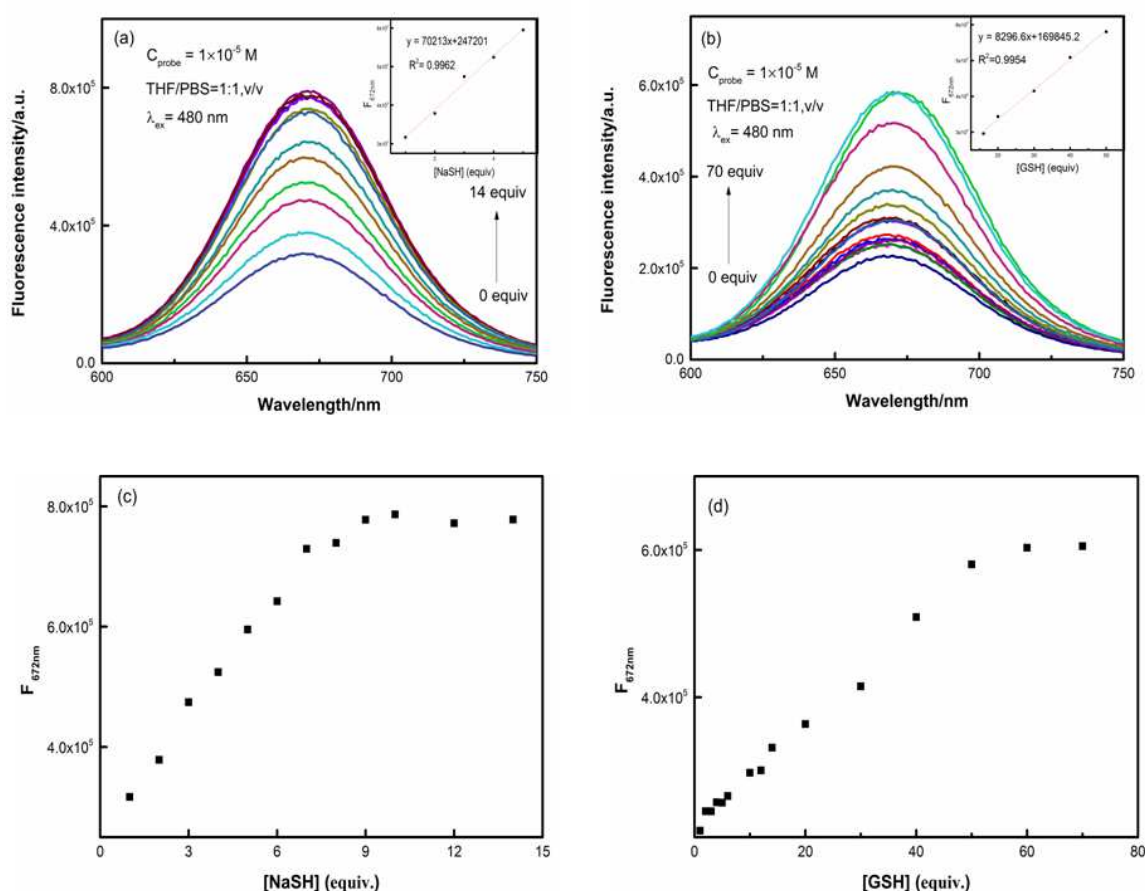


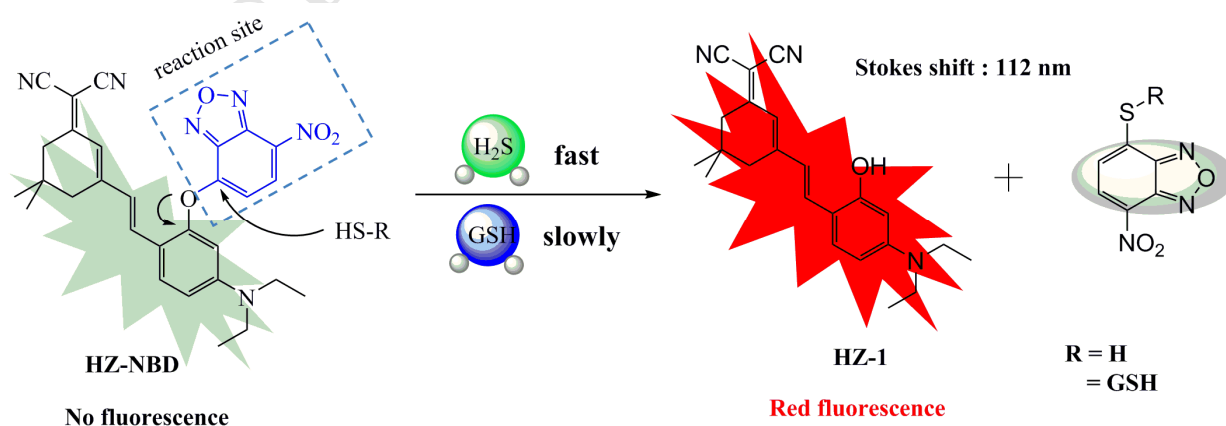
Fig. 3(a)/(b) Fluorescence spectra of HZ-NBD (10  $\mu$ M) to various concentrations of H<sub>2</sub>S (0-14 equiv) and GSH (0-70 equiv) in THF/PBS (v/v 1:1, pH=7.4) mixture solution. Inset: the linear plot of fluorescence intensity changes at 672 nm with the range of H<sub>2</sub>S concentrations (0-5 equiv) and GSH concentrations (16-50 equiv). (c)/(d) The corresponding fluorescence intensity changes of probe HZ-NBD (10  $\mu$ M) at 672 nm toward different concentrations of H<sub>2</sub>S (0-14 equiv)/GSH (0-70 equiv) ( $\lambda_{\text{ex}} = 480$  nm, slit: 3 /3 nm).

Then, the titration experiments were conducted on the solution of probe HZ-NBD (10  $\mu$ M) with an incremental addition of H<sub>2</sub>S/GSH. Initially, the free probe HZ-NBD exhibited an absorption band centered at 520 nm in THF/PBS (v/v 1:1, pH = 7.4) aqueous medium. Upon gradual addition of H<sub>2</sub>S/GSH, the solution of HZ-NBD displayed a red-shift from 520 nm to 560 nm in the UV spectrums accompanied by a drastic increase (seeing Fig. S3(a) and 3(b)). This can be ascribed to the removal of the NBD group from probe, which restored the parent fluorescent dye HZ-1. Meanwhile, the fluorescence spectra of HZ-NBD (10  $\mu$ M) with an increasing addition of H<sub>2</sub>S/GSH were performed. The probe itself exhibited insignificant fluorescence ( $\Phi = 0.0045$ ), upon the addition of different amounts of the H<sub>2</sub>S ( $\Phi = 0.080$ ), it

presented a distinct fluorescence intensity at 672 nm and reached the saturation state ( $\sim 36$ -fold) after adding 10 equiv.  $\text{H}_2\text{S}$ . For another, after adding incremental GSH ( $\Phi = 0.067$ ), the fluorescence emission at 672 nm was observed and achieved the maximum fluorescence intensity ( $\sim 29$ -fold) with 60 equiv. GSH. Furthermore, the fluorescence intensity changes of probe HZ-NBD at 672 nm versus the amounts of  $\text{H}_2\text{S}$  (0–14 equiv.) and GSH (0–70 equiv.) were revealed as shown in Fig. 3(c) and 3(d). The fluorescence intensity was linear to the concentration of  $\text{H}_2\text{S}$  (0–5 equiv.) and GSH (16–50 equiv.), and the detection limit ( $3\sigma/K[48]$ ) was calculated to be 13.2 nM ( $\text{H}_2\text{S}$ ) and 112 nM (GSH), respectively. These observations implied that the probe HZ-NBD showed high sensitivities toward  $\text{H}_2\text{S}$ /GSH.

### 3.4 Sensing mechanism of HZ-NBD towards $\text{H}_2\text{S}$ /GSH

Subsequently, to get better insight into the proposed mechanism (Scheme 3), the MS analysis of  $\text{H}_2\text{S}$  was performed to confirm the sensing process of probe HZ-NBD with  $\text{H}_2\text{S}$ . It was most likely happened as follows: Upon adding  $\text{H}_2\text{S}$ /GSH, the sulfhydryl group of  $\text{H}_2\text{S}$  and GSH initially attacked the 4-position of NBD, the ether bond was broken at the same time, which illustrated the occurrence of a nucleophilic aromatic substitution ( $\text{S}_{\text{N}}\text{Ar}$ ) reaction, the fluorescence was turn on. Additionally, the distinction of nucleophilicity of GSH and  $\text{H}_2\text{S}$  resulted in the diverse reaction rate. As shown in Fig. S5 and Fig. S6, the  $m/z$  peaks of 362.21871 and 219.08689 should be attributed to the decomposition products HZ-1 and NBD-SH, proving the fluorophore HZ-1 was indeed formed, which was forcefully consistent with our vision and could reasonably illustrate the sensing process of HZ-NBD to  $\text{H}_2\text{S}$ .



Scheme. 3 Proposed sensing mechanism of probe HZ-NBD towards  $\text{H}_2\text{S}$  and GSH

### 3.5 Time/ pH-dependence of HZ-NBD to H<sub>2</sub>S/GSH

The time and pH dependent experiments of the probe HZ-NBD towards H<sub>2</sub>S/GSH were carried out. Firstly, the kinetic studies were carried out (Fig. 4a). when adding NaSH, the fluorescence intensity at 672 nm showed the fastest growth rate and reached a plateau within 400 s, secondly was probe with GSH saturated in 500 s. As for Cys and Hcy, the fluorescence enhancement was insignificant. Therefore, the order of reaction rate was NaHS>GSH>Hcy>Cys, which was consistent with selective experimental results and literature reports[49]. In addition, to explore the biological application of the probe, the effect of pH (3.0 -12.0) on the fluorescence intensity was conducted. In the presence and absence of H<sub>2</sub>S and GSH, the fluorescence signal remained stable over a wide pH range from 7.0 to 10.0. It meant that the probe HZ-NBD exhibited a wide range of pH application particularly in physiological conditions.

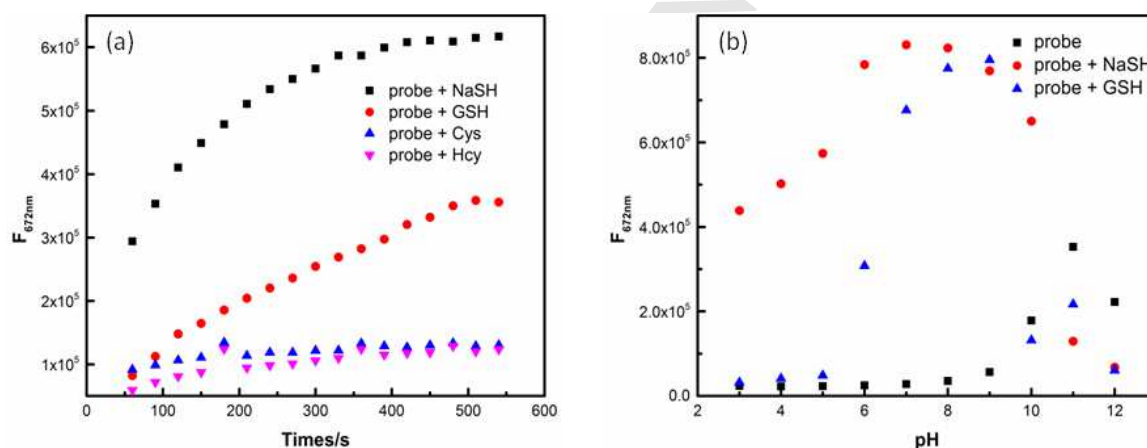


Fig. 4 (a) Time-dependent fluorescence intensity changes of HZ-NBD (10  $\mu$ M) at 672 nm upon addition of 10 equiv. of H<sub>2</sub>S, GSH, Cys and Hcy in in THF/PBS(v/v 1:1, pH=7.4) mixture solution. (b) The pH effect on the fluorescence intensity of HZ-NBD (10  $\mu$ M) at 672 nm with H<sub>2</sub>S/GSH (100  $\mu$ M) and without H<sub>2</sub>S/GSH.

### 3.6 Fluorescence imaging in living cells and cytotoxicity assay

Inspired by the above-mentioned excellent performance of the probe HZ-NBD, the applicability of the probe HZ-NBD in cellular imaging was further investigated. Before confocal fluorescence imaging, MTT assays were carried out on HZ-NBD, which indicated that probe HZ-NBD exhibited low cytotoxicity to living cells (Fig. S4). Then, cell imaging experiments were conducted in HepG2 cells. As depicted in Fig. 5, HepG2 cells were pretreated with N-ethylmaleimide (500  $\mu$ M) (NEM, a scavenger of biothiols) for 30 min followed by treated with the probe HZ-NBD (10  $\mu$ M) for another 30 min as control, no fluorescence exhibited.

There was red fluorescence shown after HepG2 cells loaded with HZ-NBD (10  $\mu\text{M}$ ) solely, this can be attributed to the existence of the endogenous  $\text{H}_2\text{S}$  and GSH. Finally, HepG2 cells were cultivated with probe (10  $\mu\text{M}$ ) for 30 min, and subsequently incubated with NEM (500  $\mu\text{M}$ ) for 30 min, GSH (200  $\mu\text{M}$ )/NaSH (200  $\mu\text{M}$ ) for another 30 min, a remarkable red fluorescence was observed. Above all, these results clearly demonstrated that the probe HZ-NBD has good biocompatibility and can serve as a fluorescent probe for sensing endogenous and exogenous  $\text{H}_2\text{S}$ /GSH in living cells.

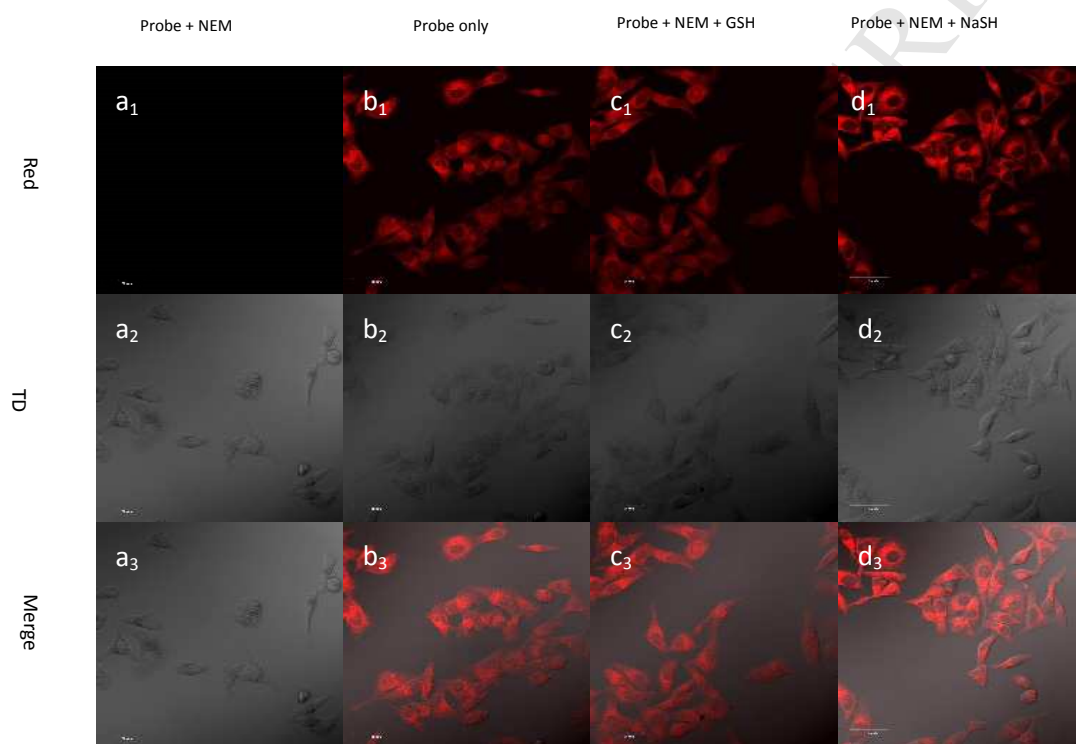


Fig. 5 Fluorescence imaging of probe HZ-NBD responding to  $\text{H}_2\text{S}$ /GSH in HepG2 cells. (a) the cells incubated with NEM (500  $\mu\text{M}$ ) for 30 min then incubated with probe (10  $\mu\text{M}$ ) for 30 min (b) the cells incubated with only probe (10  $\mu\text{M}$ ) for 30 min (c)/(d) the cells incubated with NEM (500  $\mu\text{M}$ ) for 30 min then incubated with probe (10  $\mu\text{M}$ ) for 30 min, thereafter incubated with  $\text{H}_2\text{S}$  (200  $\mu\text{M}$ )/GSH (200  $\mu\text{M}$ ) for another 30 min, respectively. ( $\lambda_{\text{ex}} = 480 \text{ nm}$ , collected at the red channel (640-720 nm)). Scale bar represents 20  $\mu\text{m}$ ).

### 3.7 Fluorescence imaging in living zebrafish

To certify that the fluorescence imaging of living bodies can be realized by HZ-NBD, the transparent zebrafish was employed. As shown in Fig.6, no fluorescence was observed when the zebrafish pretreated with NEM (500  $\mu\text{M}$ ) for 30 min were further incubated with probe HZ-NBD (10  $\mu\text{M}$ ) for another 30 min. Then, zebrafish only treated with probe HZ-NBD (10  $\mu\text{M}$ ) for 30 min, red fluorescence was displayed inside the zebrafish. Finally, when zebrafish were cultivated with probe

(10  $\mu\text{M}$ ) for 30 min, then added NEM (500  $\mu\text{M}$ ) for 30 min, GSH (200  $\mu\text{M}$ )/NaSH (200  $\mu\text{M}$ ) for another 30 min, red fluorescence emerged inside the zebrafish. It implied that probe HZ-NBD could successfully enter zebrafish and detect  $\text{H}_2\text{S}$ /GSH via a turn-on fluorescence signal response.

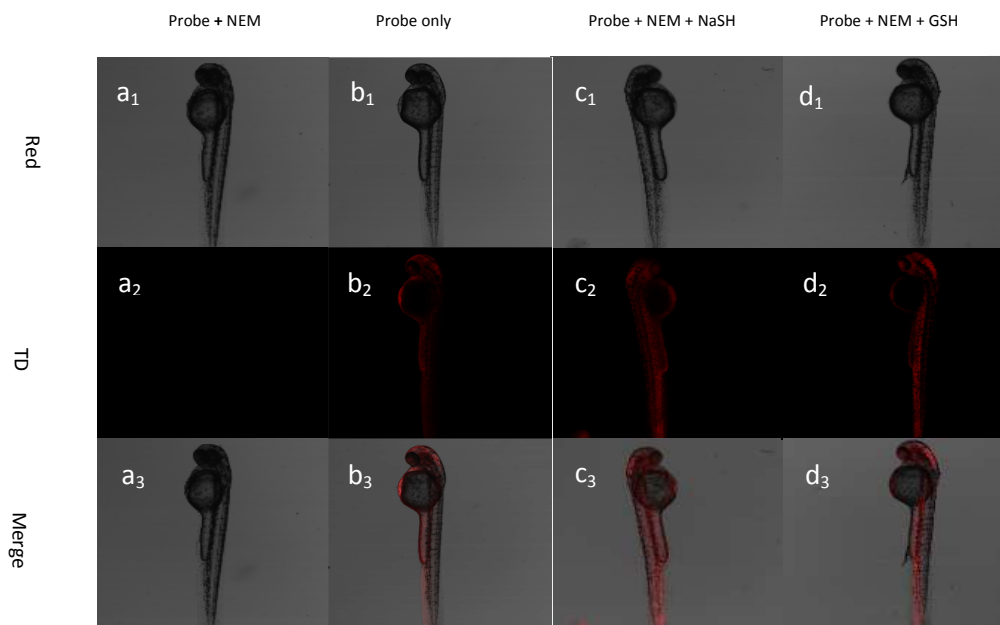


Fig. 6 Fluorescence imaging of HZ-NBD responding to  $\text{H}_2\text{S}$ /GSH in zebrafish. (a) the cells incubated with NEM (500  $\mu\text{M}$ ) for 30 min then incubated with probe (10  $\mu\text{M}$ ) for 30 min (b) the cells incubated with only probe (10  $\mu\text{M}$ ) for 30 min (c)/(d) the cells incubated with NEM (500  $\mu\text{M}$ ) for 30 min then incubated with probe (10  $\mu\text{M}$ ) for 30 min, thereafter incubated with  $\text{H}_2\text{S}$  (200  $\mu\text{M}$ )/GSH (200  $\mu\text{M}$ ) for another 30 min, respectively. ( $\lambda_{\text{ex}} = 480 \text{ nm}$ , collected at the red channel (640-720 nm)).

#### 4. Conclusion

In summary, a NIR emission fluorescent probe HZ-NBD to detect  $\text{H}_2\text{S}$  and GSH that contain isophorone-based fluorophore linked to a quenching group NBD was constructed. The probe HZ-NBD showed high selectivity toward  $\text{H}_2\text{S}$ /GSH via the sulfhydryl-promoted  $\text{S}_{\text{N}}\text{Ar}$  reaction to produce the fluorophore HZ-1 and could react with  $\text{H}_2\text{S}$  in a short time (within 7 min). Besides, the probe achieved the naked detection of  $\text{H}_2\text{S}$ /GSH, corresponding to a colour change from pink to purple red. Apart from that, the probe has many other merits such as a relatively large stokes shift ( $\lambda_{\text{em}} - \lambda_{\text{abs}} = 112 \text{ nm}$ ), a wide pH range (7~10), low cytotoxicity, biocompatibility and low detection limit for  $\text{H}_2\text{S}$  (13.2 nM) and GSH (112 nM). As a result, it can be utilized to detect  $\text{H}_2\text{S}$ /GSH in living cells and zebrafish. Taken together, the numerous advantages of HZ-NBD make it a promising prospect in biological and clinical investigations.

## Acknowledgements

We thank the financial support from the Jiangsu Ainaji Neoenergy Science & Technology Co., Ltd. (8507040091) and the Fundamental Research Funds for the Central Universities (3207045420).

## Notes and references

- [1] Kang J, Huo F, Ning P, Meng X, Chao J, Yin C. Two red-emission single and double 'arms' fluorescent materials stemmed from 'one-pot' reaction for hydrogen sulfide vivo imaging. *Sensors and Actuators B: Chemical*. 2017;250:342-50.
- [2] Zhao Q, Yin C, Kang J, Wen Y, Huo F. A viscosity sensitive azide-pyridine BODIPY-based fluorescent dye for imaging of hydrogen sulfide in living cells. *Dyes and Pigments*. 2018;159:166-72.
- [3] Huo F, Kang J, Yin C, Zhang Y, Chao J. A turn-on green fluorescent thiol probe based on the 1,2-addition reaction and its application for bioimaging. *Sensors and Actuators B: Chemical*. 2015;207:139-43.
- [4] Li J, Yin C, Zhang Y, Chao J, Huo F. A long wavelength fluorescent probe for biothiols and its application in cell imaging. *Analytical Methods*. 2016;8:6748-53.
- [5] Li D-P, Zhang J-F, Cui J, Ma X-F, Liu J-T, Miao J-Y, et al. A ratiometric fluorescent probe for fast detection of hydrogen sulfide and recognition of biological thiols. *Sensors and Actuators B: Chemical*. 2016;234:231-8.
- [6] Liu J, Chen X, Zhang Y, Gao G, Zhang X, Hou S, et al. A novel 3-hydroxychromone fluorescent probe for hydrogen sulfide based on an excited-state intramolecular proton transfer mechanism. *New Journal of Chemistry*. 2018;42:12918-23.
- [7] Wang H, Wu X, Yang S, Tian H, Liu Y, Sun B. A dual-site fluorescent probe for separate detection of hydrogen sulfide and bisulfite. *Dyes and Pigments*. 2019;160:757-64.
- [8] HIDEO KIMURA YN, KEN UMEMURA, and YUKA KIMURA. Physiological Roles of Hydrogen Sulfide: Synaptic Modulation, Neuroprotection, and Smooth Muscle Relaxation. *ANTIOXIDANTS & REDOX SIGNALING*. 2005;7:795-803.
- [9] Hughes MN, Centelles MN, Moore KP. Making and working with hydrogen sulfide: The chemistry and generation of hydrogen sulfide in vitro and its measurement in vivo: a review. *Free radical biology & medicine*. 2009;47:1346-53.
- [10] He L, Yang X, Xu K, Kong X, Lin W. A multi-signal fluorescent probe for simultaneously distinguishing and sequentially sensing cysteine/homocysteine, glutathione, and hydrogen sulfide in living cells. *Chem Sci*. 2017;8:6257-65.
- [11] Xie JY, Li CY, Li YF, Fei J, Xu F, Ou-Yang J, et al. Near-Infrared Fluorescent Probe with High Quantum Yield and Its Application in the Selective Detection of Glutathione in Living Cells and Tissues. *Analytical chemistry*. 2016;88:9746-52.
- [12] Wang J, Niu L, Huang J, Yan Z, Zhou X, Wang J. Thiazolyl substituted NBD as fluorescent probe for the detection of homocysteine and cysteine. *Dyes and Pigments*. 2018;158:151-6.
- [13] Cao M, Chen H, Chen D, Xu Z, Liu SH, Chen X, et al. Naphthalimide-based fluorescent probe for selectively and specifically detecting glutathione in the lysosomes of living cells. *Chemical communications*. 2016;52:721-4.
- [14] Yang B, Su M-M, Xue Y-S, He Z-X, Xu C, Zhu H-L. A selective fluorescence probe for H<sub>2</sub>S from biothiols with a significant regioselective turn-on response and its application for H<sub>2</sub>S detection in living cells and in living *Caenorhabditis elegans*. *Sensors and Actuators B: Chemical*. 2018;276:456-65.

- [15] Chen S, Hou P, Wang J, Fu S, Liu L. A rapid and selective fluorescent probe with a large Stokes shift for the detection of hydrogen sulfide. *Spectrochimica acta Part A, Molecular and biomolecular spectroscopy*. 2018;203:258-62.
- [16] Wang Zhang GW, Tian Cheng, Bingxiang Wang, Yuliang Jiang, Shen aJ. A novel near-infrared and naked-eyes turn on fluorescent probe for detection of biothiols with a large Stokes shift and its application in living cells. *Analytical Methods*. 2018;10:3991-9.
- [17] Zhang H, Liu R, Liu J, Li L, Wang P, Yao SQ, et al. A minimalist fluorescent probe for differentiating Cys, Hcy and GSH in live cells. *Chem Sci*. 2016;7:256-60.
- [18] Chen Q, Yang J, Li Y, Zheng J, Yang R. Sensitive and rapid detection of endogenous hydrogen sulfide distributing in different mouse viscera via a two-photon fluorescent probe. *Analytica chimica acta*. 2015;896:128-36.
- [19] Zhao Q, Huo F, Kang J, Zhang Y, Yin C. A novel FRET-based fluorescent probe for the selective detection of hydrogen sulfide (H<sub>2</sub>S) and its application for bioimaging. *Journal of Materials Chemistry B*. 2018;6:4903-8.
- [20] Niu LY, Guan YS, Chen YZ, Wu LZ, Tung CH, Yang QZ. BODIPY-based ratiometric fluorescent sensor for highly selective detection of glutathione over cysteine and homocysteine. *Journal of the American Chemical Society*. 2012;134:18928-31.
- [21] Ren X, Wang F, Lv J, Wei T, Zhang W, Wang Y, et al. An ESIPT-based fluorescent probe for highly selective detection of glutathione in aqueous solution and living cells. *Dyes and Pigments*. 2016;129:156-62.
- [22] Li J, Yin C, Huo F. Chromogenic and fluorogenic chemosensors for hydrogen sulfide: review of detection mechanisms since the year 2009. *RSC Advances*. 2015;5:2191-206.
- [23] Kang J, Huo F, Yin C. A novel ratiometric fluorescent H<sub>2</sub>S probe based on tandem nucleophilic substitution/cyclization reaction and its bioimaging. *Dyes and Pigments*. 2017;146:287-92.
- [24] Jun Yin YK, Dabin Kim, Dayoung Lee, Gyoungmi Kim, Ying Hu,, Ji-Hwan Ryu aJY. Cyanine-Based Fluorescent Probe for Highly Selective Detection of Glutathione in Cell Cultures and Live Mouse Tissues. *J Am Chem Soc*. 2014;136:5351-8.
- [25] Yang Y, Yin C, Huo F, Zhang Y, Chao J. A ratiometric colorimetric and fluorescent chemosensor for rapid detection hydrogen sulfide and its bioimaging. *Sensors and Actuators B: Chemical*. 2014;203:596-601.
- [26] Li X, Huo F, Yue Y, Zhang Y, Yin C. A coumarin-based "off-on" sensor for fluorescence selectively discriminating GSH from Cys/Hcy and its bioimaging in living cells. *Sensors and Actuators B: Chemical*. 2017;253:42-9.
- [27] Ou-Yang J, Li C-Y, Li Y-F, Fei J, Xu F, Li S-J, et al. A rhodamine-based fluorescent probe with high water solubility and its application in the detection of glutathione with unique specificity. *Sensors and Actuators B: Chemical*. 2017;240:1165-73.
- [28] Chen W, Luo H, Liu X, Foley JW, Song X. Broadly Applicable Strategy for the Fluorescence Based Detection and Differentiation of Glutathione and Cysteine/Homocysteine: Demonstration in Vitro and in Vivo. *Analytical chemistry*. 2016;88:3638-46.
- [29] Xiong J, Xia L, Huang Q, Huang J, Gu Y, Wang P. Cyanine-based NIR fluorescent probe for monitoring H<sub>2</sub>S and imaging in living cells and in vivo. *Talanta*. 2018;184:109-14.
- [30] Xia X, Qian Y, Shen B. Synthesis of a BODIPY disulfonate near-infrared fluorescence-enhanced probe with high selectivity to endogenous glutathione and two-photon fluorescent turn-on through thiol-induced SNAr substitution. *Journal of Materials Chemistry B*. 2018;6:3023-9.

- [31] Li H, Peng W, Feng W, Wang Y, Chen G, Wang S, et al. A novel dual-emission fluorescent probe for the simultaneous detection of H<sub>2</sub>S and GSH. *Chemical communications*. 2016;52:4628-31.
- [32] Chen F, Han D, Liu H, Wang S, Li KB, Zhang S, et al. A tri-site fluorescent probe for simultaneous sensing of hydrogen sulfide and glutathione and its bioimaging applications. *The Analyst*. 2018;143:440-8.
- [33] Hong J, Feng W, Feng G. Highly selective near-infrared fluorescent probe with rapid response, remarkable large Stokes shift and bright fluorescence for H<sub>2</sub>S detection in living cells and animals. *Sensors and Actuators B: Chemical*. 2018;262:837-44.
- [34] Jiao X, Liu C, He S, Zhao L, Zeng X. Highly selective and sensitive ratiometric near-infrared fluorescent probe for real-time detection of Hg<sup>2+</sup> and its bioapplications in live cells. *Dyes and Pigments*. 2019;160:86-92.
- [35] Zhang W, Zhao X, Gu W, Cheng T, Wang B, Jiang Y, et al. A novel naphthalene-based fluorescent probe for highly selective detection of cysteine with a large Stokes shift and its application in bioimaging. *New Journal of Chemistry*. 2018;42:18109-16.
- [36] Zhong K, Deng L, Zhao J, Yan X, Sun T, Li J, et al. A novel near-infrared fluorescent probe for highly selective recognition of hydrogen sulfide and imaging in living cells. *RSC Advances*. 2018;8:23924-9.
- [37] Kang J, Huo F, Zhang Y, Chao J, Glass TE, Yin C. A novel near-infrared ratiometric fluorescent probe for cyanide and its bioimaging applications. *Spectrochimica acta Part A, Molecular and biomolecular spectroscopy*. 2018;209:95-9.
- [38] Wang L, Zhuo S, Tang H, Cao D. A near-infrared turn on fluorescent probe for cysteine based on organic nanoparticles. *Sensors and Actuators B: Chemical*. 2018;277:437-44.
- [39] Wang SP, Deng WJ, Sun D, Yan M, Zheng H, Xu JG. A colorimetric and fluorescent merocyanine-based probe for biological thiols. *Organic & biomolecular chemistry*. 2009;7:4017-20.
- [40] Zhang X, Chen Y. Synthesis and fluorescence of dicyanoisophorone derivatives. *Dyes and Pigments*. 2013;99:531-6.
- [41] Zhang W, Huo F, Yin C. Recent advances of dicyano-based materials in biology and medicine. *Journal of Materials Chemistry B*. 2018;6:6919-29.
- [42] Huo F, Zhang Y, Ning P, Meng X, Yin C. A novel isophorone-based red-emitting fluorescent probe for selective detection of sulfide anions in water for in vivo imaging. *Journal of Materials Chemistry B*. 2017;5:2798-803.
- [43] Gao X, Li X, Li L, Zhou J, Ma H. A simple fluorescent off-on probe for the discrimination of cysteine from glutathione. *Chemical communications*. 2015;51:9388-90.
- [44] Li X, Zhang X, Ma H, Wu D, Zhang Y, Du B, et al. Cathodic electrochemiluminescence immunosensor based on nanocomposites of semiconductor carboxylated g-C<sub>3</sub>N<sub>4</sub> and graphene for the ultrasensitive detection of squamous cell carcinoma antigen. *Biosensors & bioelectronics*. 2014;55:330-6.
- [45] Zhang L, Li S, Hong M, Xu Y, Wang S, Liu Y, et al. A colorimetric and ratiometric fluorescent probe for the imaging of endogenous hydrogen sulphide in living cells and sulphide determination in mouse hippocampus. *Organic & biomolecular chemistry*. 2014;12:5115-25.
- [46] Ding S, Feng W, Feng G. Rapid and highly selective detection of H<sub>2</sub>S by nitrobenzofurazan (NBD) ether-based fluorescent probes with an aldehyde group. *Sensors and Actuators B: Chemical*. 2017;238:619-25.
- [47] Zhang W, Liu J, Yu Y, Han Q, Cheng T, Shen J, et al. A novel near-infrared fluorescent probe for highly selective detection of cysteine and its application in living cells. *Talanta*. 2018;185:477-82.
- [48] Xia X, Qian Y. NIR two-photon fluorescent probe for biothiol detection and imaging of living cells in vivo. *The Analyst*. 2018;143:5218-24.
- [49] Zhang J, Ji X, Zhou J, Chen Z, Dong X, Zhao W. Pyridinium substituted BODIPY as NIR fluorescent probe for simultaneous sensing of hydrogen sulphide/glutathione and cysteine/homocysteine. *Sensors and Actuators B: Chemical*. 2018;257:1076-82.

ACCEPTED MANUSCRIPT

## Highlight

1. Near infrared emission at 672 nm.
2. Distinguish H<sub>2</sub>S and GSH simultaneously over Hcy and Cys.
3. Fluorescence imaging in zebrafish/cells in vivo and vitro.
4. High sensitivity (13.2 nM for H<sub>2</sub>S, 112.0 nM for GSH) and selectivity.